Since January 2020 Elsevier has created a COVID-19 resource centre with free information in English and Mandarin on the novel coronavirus COVID-19. The COVID-19 resource centre is hosted on Elsevier Connect, the company's public news and information website.

Antiviral Research 160 (2018) 183–189

Contents lists available at ScienceDirect

Antiviral Research

journal homepage: www.elsevier.com/locate/antiviral

Seneca Valley Virus 3C protease negatively regulates the type I interferon pathway by acting as a viral deubiquitinase

Qiao Xue[a], Huisheng Liu[a], Zixiang Zhu[a], Fan Yang[a], Qinghong Xue[b], Xuepeng Cai[b], Xiangtao Liu[a], Haixue Zheng[a,*]

[a] State Key Laboratory of Veterinary Etiological Biology, National Foot and Mouth Diseases Reference Laboratory, Key Laboratory of Animal Virology of Ministry of Agriculture, Lanzhou Veterinary Research Institute, Chinese Academy of Agricultural Sciences, Lanzhou, 730046, China
[b] China Institute of Veterinary Drug Control, Beijing, 100081, China

ARTICLE INFO

Keywords:
Deubiquitinase
Innate immunity
Seneca valley virus
Ubiquitin
3C-like protease

ABSTRACT

The mechanisms that enable Seneca Valley Virus (SVV) to escape the host innate immune response are not well known. Previous studies demonstrated that SVV $3C^{pro}$ suppresses innate immune responses by cleavage of host proteins and degradation of IRF3 and IRF7 protein expression. Here, we showed that SVV 3C protease ($3C^{pro}$) has deubiquitinating activity. Overexpressed $3C^{pro}$ inhibits the ubiquitination of cellular substrates, acting on both lysine-48- and lysine-63-linked polyubiquitin chains. SVV infection also possessed deubiquitinating activity. The ubiquitin-proteasome system was significantly involved in SVV replication. Furthermore, $3C^{pro}$ inhibited the ubiquitination of retinoic acid-inducible gene I (RIG-I), TANK-binding kinase 1 (TBK1), and TNF receptor-associated factor 3 (TRAF3), thereby blocking the expression of interferon (IFN)-β and IFN stimulated gene 54 (ISG54) mRNAs. A detailed analysis revealed that mutations (H48A, C160A, or H48A/C160A) that ablate the Cys and His residues of $3C^{pro}$ abrogated its deubiquitinating activity and the ability of $3C^{pro}$ to block IFN-β induction.

Together, our results demonstrate a novel mechanism developed by SVV $3C^{pro}$ to promote viral replication, and may also provide a novel strategy for improving ubiquitination-based therapy.

Seneca Valley Virus (SVV), belonging to the *Picornaviridae*, is a positive-sense, single-stranded RNA virus that is most closely related to *Cardiovirus* (Hales et al., 2008). SVV was first isolated in the United States in 2002 as a contaminant in the cell culture of human fetal retinoblasts (Segales et al., 2017). Afterward, a large number of SVV infections, which were characterized by porcine idiopathic vesicular disease, were observed in the United States, Canada, Brazil, and China (Xue et al., 2018). In China, the first case of SVV infection was identified in Guangdong Province in 2015 (Wu et al., 2016). Subsequently, new SVV isolates were identified in Guangdong and Hubei Provinces (Qian et al., 2017; Zhao et al., 2017). In 2017, we also identified a novel SVV strain in Fujian Province in China (Zhu et al., 2017).

Many viruses have evolved strategies to evade innate immune response by inhibiting the host ubiquitination to promote their survival. For instance, human immunodeficiency virus-1 inhibits the antiviral response by the ub-mediated degradation of IRF3 (Okumura et al., 2008), porcine reproductive and respiratory syndrome (PRRS) virus inhibits nuclear factor kappa-light-chain-enhancer of activated B cells (NF-κB) activation by inhibition of the polyubiquitination process of IκBα (Sun et al., 2010). To date, SVV $3C^{pro}$ has evolved mechanism to cleave or degrade innate immune adaptors to escape the host antiviral innate immune response (Qian et al., 2017; Xue et al., 2018). However, other mechanisms that enable SVV to escape the host innate immune response remain unclear.

To determine whether SVV can evade innate immune response by inhibiting the host ubiquitination, HEK293T cells were transfected with FLAG-tagged VP1, VP2, 2AB, 2B, 2C, 3D, 3C plasmids along with HA-Ub plasmid. At 24 h post-transfection (hpt), the ubiquitinated cellular proteins was assessed by western blotting. The SVV 2A, 2C, and $3C^{pro}$ inhibited the level of ubiquitinated cellular proteins, and $3C^{pro}$ most significantly inhibited this process (Supplementary Fig. 1). Human DUBs are classified into five subfamilies based on their catalytic domains structures. They have a high degree of homology in the two regions known as Cys and His boxes that surround the catalytic Cys and His residues (Nijman et al., 2005). Similar to other picornaviruses, SVV $3C^{pro}$ also possesses a conserved catalytic box with Cys and His residues (Qian et al., 2017). Therefore, the SVV $3C^{pro}$ was selected for further studies. To determine whether $3C^{pro}$ functions as a DUB, HEK293T cells were transfected with increasing amounts of plasmid encoding $3C^{pro}$ along with HA-Ub or empty vector. At 24 hpt, the effect of $3C^{pro}$ on all

* Corresponding author.
E-mail address: haixuezheng@163.com (H. Zheng).

https://doi.org/10.1016/j.antiviral.2018.10.028
Received 13 July 2018; Received in revised form 26 September 2018; Accepted 31 October 2018
Available online 05 November 2018

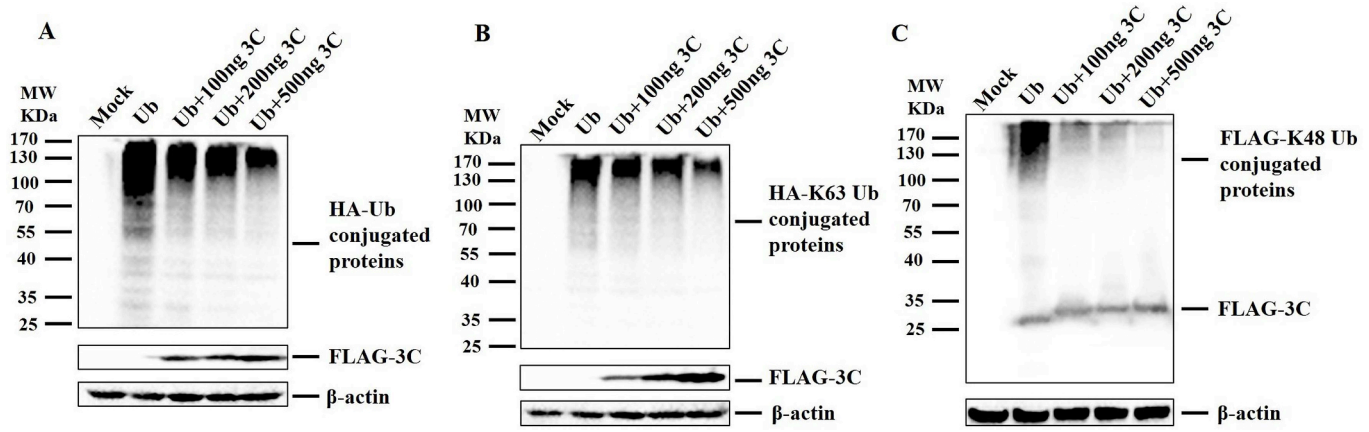

Fig. 1. SVV 3C^{pro} has DUB activity. HEK-293T cells were seeded in six-well plates and the monolayer cells were transfected with 1 μg HA-Ub-, HA-K63-Ub-, or FLAG-K48-Ub-expressing plasmids along with 0.1, 0.2, or 0.5 μg FLAG-3C-expressing plasmid. The empty FLAG vector was used in the transfection process to ensure that the same number of cells received the same amount of total plasmids. At 24 hpt, the levels of Ub (A)-, K63 (B)-, and K48 (C)-linked cellular proteins were detected by western blotting.

ubiquitinated cellular proteins was assessed by western blotting. As shown in Fig. 1A, expression of 3C^{pro} resulted in a dose-dependent reduction of the level of ubiquitinated cellular proteins compared with that in the empty vector-transfected cells. To further determine which Ub linkage type is targeted by 3C^{pro}, HEK293T cells were transfected with HA-K63-Ub or FLAG-K48-Ub in lieu of HA-Ub. At 24 hpt, the cells were collected for western blotting. Both K48- and K63-linked Ub chains were also processed by 3C^{pro} in a dose-dependent manner (Fig. 1 B and C).

We also analyzed DUB activity during SVV infection. HEK293T cells were mock infected or infected with SVV at a multiplicities of infection (MOI) of 3 for 12 h. As shown in Fig. 2 A, the levels of endogenous Ub, K48, and K63 ubiquitinated cellular proteins were reduced in SVV-infected cells compared to those in uninfected cells. Taken together, these results confirm that SVV exerts DUB activity during viral infection and 3C^{pro} is a potent viral DUB that inhibits Ub conjugates formed through K48 or K63 linkages in cellular substrates.

SVV 3C^{pro} contains Cys and His residues. Therefore, the three mutants, namely the single-site mutants H48A or C160A, and the double-sites mutants H48A/C160A (3Cdm) (Xue et al., 2018), were used to confirm whether the Cys and His residues are involved in the DUB activity of SVV 3C^{pro}. HEK293T cells were co-transfected with HA-Ub-, HA-K63-Ub-, and FLAG-K48-Ub-expressing plasmids along with FLAG-3C-expressing plasmid or FLAG-3C mutants expressing plasmids. At 24 hpt, the cells were collected for western blotting. All the 3C^{pro} proteins without Cys and His residues lost the ability to inhibit Ub conjugates compared with the overexpression of wild-type SVV 3C^{pro} (3Cwt) (Fig. 3 A–C).

To further confirm the DUB activity of SVV 3C^{pro}, HEK293T cells were transfected with FLAG-3C-expressing plasmid, FLAG-3Cdm expressing plasmid, or empty vector. At 24 hpt, the cells were collected for western blotting. It showed that the 3C^{pro} proteins without Cys and His residues could no longer reduce levels of endogenous ubiquitinated Ub, K48, and K63 (Fig. 2 B). Taken together, these results indicate that the catalytic Cys and His residues of SVV 3C^{pro} are required for its DUB activity.

We also investigated whether 3C^{pro} is associated with the deubiquitination of RIG-I, TBK1, and TRAF3. To do so, HEK293T cells cultured in 10-cm dishes were transfected with various plasmids. At 32 hpt, cell lysates were immunoprecipitated with anti-FLAG or anti-Myc antibody and analyzed by western blotting. Overexpression of 3Cwt significantly inhibited the ubiquitination of RIG-I (Fig. 4A), TBK1 (Fig. 4B), and TRAF3 (Fig. 4C). Overexpression of 3Cdm, which lacks DUB activity, had no such effects. In addition, our results also demonstrated an interaction between 3C^{pro} and either TBK1, or TRAF3 (Fig. 4B and C). To investigate the interaction between 3C^{pro} and RIG-I, HEK293T cells were transfected with FLAG-3C-expressing plasmid or empty vector. At 32 hpt, cell lysates were immunoprecipitated with anti-RIG-I antibody and analyzed by western blotting. RIG-I pulled down FLAG-3C (Fig. 4D), which confirmed that 3C^{pro} interacted with RIG-I.

The interaction of 3C^{pro} and RIG-I, TBK1, or TRAF3 in context of viral infection was further confirmed. HEK293T cells were mock-infected or infected with SVV (MOI 1) for 12 h. The cell lysates were immunoprecipitated with anti-3C antibody and subjected to immunoblotting analysis. 3C^{pro} pulled down RIG-I, TBK1, and TRAF3 in SVV-infected cells (Fig. 4E). A reverse immunoprecipitation experiment was subsequently performed using anti-RIG-I, TBK1, or TRAF3 antibody, which showed that RIG-I, TBK1, or TRAF3 also immunoprecipitated 3C^{pro} (Fig. 4F). These results indicate that the interaction of 3C^{pro} with RIG-I, TBK1, and TRAF3 in the context of viral infection is involved in the suppression of ubiquitination levels.

Endogenous ubiquitination levels of RIG-I, TBK1, and TRAF3 in SVV-infected cells were further assessed. HEK293T cells were mock infected or infected with SVV (MOI 3) for 12 h. Cell lysates were immunoprecipitated with anti-RIG-I, TBK1, or TRAF3 antibody and analyzed by western blotting. The results showed that the ubiquitination levels of endogenous K48 for TBK1, and K63 for RIG-I and TRAF3 were reduced during SVV infection (Fig. 4G). Taken together, these results indicate that SVV and 3C^{pro} inhibit the ubiquitination of RIG-I, TBK1, and TRAF3 in a DUB-dependent manner.

Ubiquitination and deubiquitination are important mechanisms that are involved in regulating type I IFN signaling pathways (Peisley et al., 2014). To date, many cellular Ub ligase enzymes can regulate these processes. For example, the E3 ubiquitin ligase RNF128 or Nrdp1 directly enhance ubiquitination of TBK1, which facilitates the activation of TBK1 (Song et al., 2016; Wang et al., 2009). Meanwhile, many cellular DUBs negatively regulate type I IFN signaling pathways. For example, USP3, USP38, and USP19 target RIG-I, TBK1, and TRAF3 for deubiquitination, respectively, thereby blocking the activation of type I IFN signaling pathways (Cui et al., 2014; Gu et al., 2017; Lin et al., 2016). DUB activity also has been demonstrated in many bacteria and viruses, such as *Salmonella enterica* serovar Typhimurium, FMDV, PRRSV, herpesviruses, coronaviruses, and bunyaviruses, and DUB

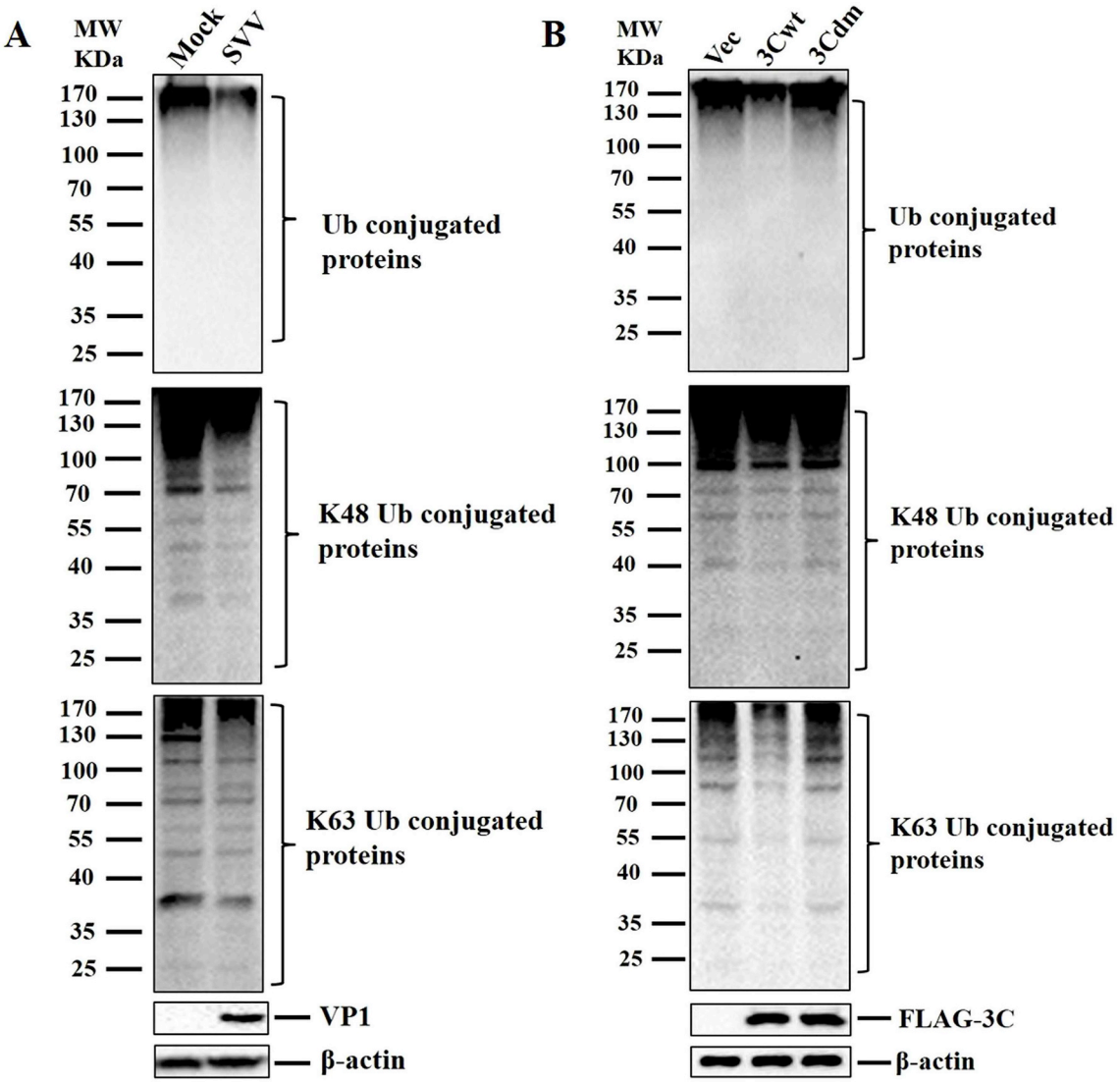

Fig. 2. SVV exerts DUB activity during viral infection. (A) HEK-293T cells were seeded in six-well plates, and the monolayer cells were mock infected or infected with SVV (MOI = 3) for 12 h. The levels of endogenous Ub-, K63-, and K48-linked cellular proteins were detected by western blotting. (B) HEK-293T cells were seeded in six-well plates, and the monolayer cells were transfected with 1 μg FLAG-3Cwt-expressing plasmid, FLAG-3Cdm-expressing plasmid, or empty vector. At 24 hpt, The levels of endogenous Ub-, K63-, and K48-linked cellular proteins were detected by western blotting.

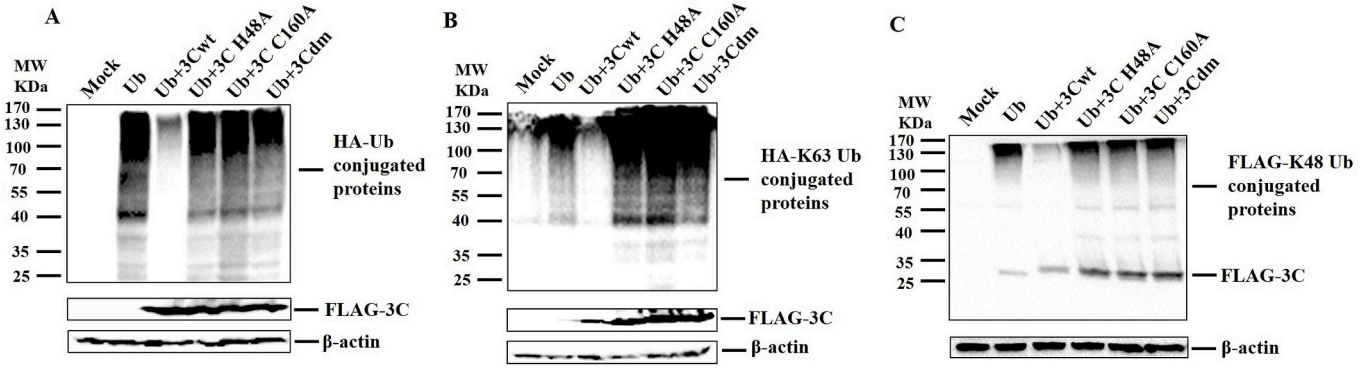

Fig. 3. SVV $3C^{pro}$ inhibits the ubiquitination of cellular proteins in a manner that is dependent on its DUB activity. (A) HEK-293T cells were seeded in six-well plates, and the monolayer cells were transfected with 1 μg HA-Ub-expressing plasmid along with 1 μg FLAG-3Cwt-expressing plasmid, 1 μg FLAG-3C H48A-expressing plasmid, 1 μg FLAG-3C C160A-expressing plasmid, or 1 μg FLAG-3Cdm-expressing plasmid. The empty FLAG vector was used in the transfection process to ensure that the same number of cells received the same amount of total plasmids. At 24 hpt, the cells were collected for western blotting. Similar transfection and analysis were performed for K63-Ub (B) and K48-Ub (C) as described above.

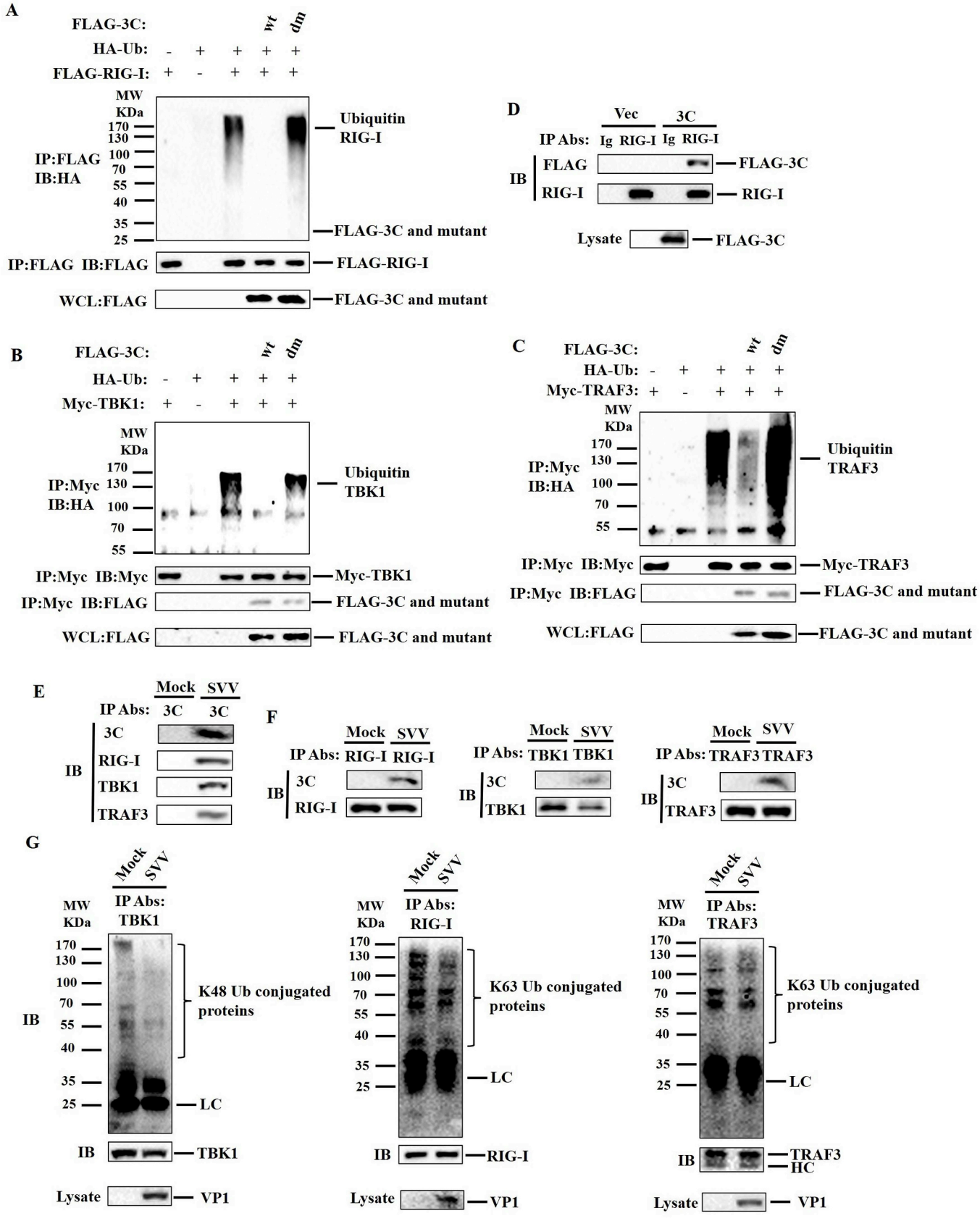

(caption on next page)

Fig. 4. SVV 3C^{pro} inhibits the ubiquitination of RIG-I, TBK1, and TRAF3. HEK-293T cells were seeded in 100-mm dishes, and the monolayer cells were co-transfected with 2 μg HA-Ub-expressing plasmid, 1 μg FLAG-3Cwt-expressing plasmid, 1 μg FLAG-3Cdm-expressing plasmid, and the RIG-I (A), TBK1 (B), or TRAF3 (C) expression plasmids (4 μg). MG132 (20 nM) was added at 30 hpt. Cell lysates were prepared at 2 h after treatment and immunoprecipitated with anti-FLAG or anti-Myc antibody, and the Ub conjugation of the proteins was detected by western blotting with anti-HA antibody. The input tagged proteins were detected with the indicated antibodies. (D) HEK-293T cells were seeded in 100-mm dishes, and the monolayer cells were transfected with 5 μg FLAG-3C-expressing plasmid or empty vector. At 32 hpt, cell lysates were immunoprecipitated with anti-RIG-I antibody and analyzed by western blotting. The whole-cell lysates and IP antibody-antigen complexes were analyzed by IB using anti-FLAG and anti-RIG-I antibodies. (E, F) HEK-293T cells were seeded in 100-mm dishes, and the monolayer cells were mock-infected or infected with SVV (MOI 1) for 12 h. Cell lysates were immunoprecipitated with anti-3C antibody and analyzed by western blotting (E). Similar infection and IP experiments were carried out as described above. However, the lysates were immunoprecipitated with anti-RIG-I, TBK1, or TRAF3 antibody and subjected to western blotting (F). (G) HEK293T cells were cultured in 10-cm dishes, and the monolayer cells were mock infected or infected with SVV (MOI 3) for 12 h. Cell lysates were immunoprecipitated with anti-TBK1, RIG-I, or TRAF3 antibody and analyzed by western blotting. The whole-cell lysates and IP antibody-antigen complexes were analyzed by IB using anti-K48, K63, TBK1, RIG-I, TRAF3, or VP1 antibodies. HC represents heavy chain. LC represents light chain.

Table 1
The qPCR primers used in this study.

Primers	Sequences (5′-3′)	Target gene
hIFN-β-F	GACATCCCTGAGGAGATTAAG	human IFN-β gene
hIFN-β-R	ATGTTCTGGAGCATCTCATAG	
hISG54-F	ACGGTATGCTTGGAACGATTG	human ISG54 gene
hISG54-R	AACCCAGAGTGTGGCTGATG	
hISG56-F	CTTGAGCATCCTCGGGTTCATC	human ISG56 gene
hISG56-R	AAGTCAGCAGCCAGGTTTAGGG	
SVV-F	AGAATTTGGAAGCCATGCTCT	SVV gene
SVV-R	GAGCCAACATAGARACAGATTGC	
hGAPDH-F	CGGGAAGCTTGTGATCAATGG	human GAPDH gene
hGAPDH-R	GGCAGTGATGGCATGGACTG	

enzymes play multiple roles in regulating bacterial or viral infections (Fiskin et al., 2016; Sun et al., 2010; van Wijk et al., 2017; Wang et al., 2011). Here, SVV 3C^{pro} also has DUB activity. To investigate whether SVV 3C^{pro} can block the type I IFN signaling pathway, quantitative polymerase chain reaction (qPCR) analysis was performed to determine the transcript levels of the IFN-β, ISG54, and ISG56 genes during viral infection. Relative expression of mRNA was calculated based on the comparative cycle threshold (CT) ($2^{-\Delta\Delta CT}$) method (Schmittgen and Livak, 2008). The qPCR primers used in this study are listed in Table 1. It showed that only FLAG-3Cwt was able to inhibit SeV-induced IFN-β, ISG54, and ISG56 mRNA expression (Fig. 5A).

To determine whether 3C^{pro} affected the replication of SVV, HEK293T cells were seeded in 6-well plates, and the monolayer cells were transfected with FLAG–3C-expressing plasmid or empty vector. At 24 hpt, the cells were infected with equal amounts of SVV (MOI 1). At 12 h post-infection (hpi), viral RNA and protein levels were examined. Overexpression of 3C^{pro} significantly enhanced replication of SVV (Fig. 5B).

The ubiquitin-proteasome system (UPS) plays important roles in the degradation of proteins, the immune response, and signal transduction (Casorla-Perez et al., 2017). The UPS is a double-edged sword in viral pathogenesis: the UPS is necessary for many viruses replication by maintaining the proper functions of viral proteins (Barrado-Gil et al., 2017; Luo, 2016; Wang et al., 2016); the UPS can constitute host immune system to reduce viral replication (Luo, 2016). For example, the UPS was essential for coronavirus replication (Raaben et al., 2010), whereas coronavirus papain-like proteases can act as DUBs that block type I IFN production (Clementz et al., 2010). Proteasome inhibitors MG132 can inhibit the UPS. To determine the impact of the UPS on the replication of SVV, HEK293T cells were infected with an equal amount of SVV (MOI 1). At 4 hpi, the cells were incubated with or without MG132 for 8 h. Viral RNA and protein levels were examined. MG132 significantly inhibited replication of SVV (Fig. 5C), which indicated that the UPS was also essential for SVV replication. Therefore, we speculated that the UPS plays an important role in maintaining functions of SVV proteins.

The abundance of RIG-I, TBK1, and TRAF3 during SVV infection remained unclear. HEK293T cells cultured in 6-well plates were mock infected or infected with SVV. The abundance of RIG-I, TBK1, and TRAF3 were compared at 0, 6, and 12 h after SVV infection. The results showed that SVV infection had no impact on the abundance of RIG-I and TRAF3, but did inhibit expression of TBK1 (Fig. 5D). It is well known that reduction of the K48-linked polyubiquitin can stabilize TBK1. However, our results indicated that SVV or 3C^{pro} reduced expression of TBK1. To clarify this unexpected result, a broad-range deubiquitinase inhibitor, PR-619 (Sigma-Aldrich), was selected for further study (Altun et al., 2011). The ubiquitination levels of endogenous K48 for TBK1 was enhanced after PR-619 incubation (Supplementary Fig.2). HEK293T cells were transfected with FLAG–3C-expressing plasmid or infected with SVV (MOI 1). Then, the cells were treated with or without PR-619. Cell lysates were analyzed by western blotting. The expression of TBK1 in the 3C^{pro}-transfected and SVV-infected cells was enhanced comparing with that in the PR-619-treated cells (Fig. 5E), which indicated that 3C-induced reduction of the K48-linked polyubiquitin of TBK1 enhanced the expression of TBK1. However, as a whole, 3C^{pro} and SVV still reduced the expression of TBK1. SVV 3C^{pro} possesses protease activity. Therefore, we speculated that 3C^{pro} reduced the expression of TBK1 by its protease activity, and 3C^{pro} partly stabilized TBK1 by its DUB activity.

To further investigate whether SVV 3C^{pro} can block RIG-I- and TBK1-induced type I IFN signaling pathway, we performed a luciferase reporter assay. HEK293T cells grown in 24-well plates were co-transfected with 0.1 μg/well of the plasmid IFN-β-Luciferase (IFN-β-Luc) along with 0.01 μg/well of plasmid pRL-TK and plasmids encoding FLAG-RIG-I, Myc-TBK1, FLAG-3Cwt, FLAG-3Cdm, or empty vector. At 24 hpt, the cells were lysed and analyzed with a Dual-specific Luciferase Assay kit. As shown in Fig. 5F, RIG-I-, and TBK1-mediated IFN-β promoter activity was reduced in the presence of FLAG-3Cwt but not FLAG-3Cdm. To further confirm this effect, we conducted a qPCR analysis to determine the levels of the RIG-I- and TBK1-mediated endogenous transcription of the IFN-β and ISG54 genes. The results showed that FLAG-3Cwt also inhibits RIG-I- and TBK1-induced IFN-β and ISG54 mRNA expression (Fig. 5G), which is in accordance with previous findings showing that SVV 3C^{pro} significantly inhibited the endogenous transcription of the IFN-β and ISG56 genes that is mediated by RIG-I and TBK1 (Qian et al., 2017). Taken together, these results indicate that SVV 3C^{pro} promotes replication of SVV and suppresses RIG-I- and TBK1-induced type I IFN production in a manner that is dependent on its DUB activity.

In the present study, we provide direct evidence that SVV 3C^{pro} is a novel viral deubiquitinating enzyme. However, more work will be required to determine if other picornavirus 3C^{pro}, such as encephalomyocarditis virus, enterovirus 71, coxsackievirus A16, or FMDV, have DUB activity. Our data also uncover a novel mechanism by which SVV 3C^{pro} antagonizes type I IFN induction, i.e., by deubiquitinating the critical signaling moleculars RIG-I, TBK1, and TRAF3. Our results comparing various 3C^{pro} mutants suggest that the DUB activity of 3C^{pro} enables it to block induction of the IFN-β promoter and the

endogenous transcription of the IFN-β and ISG54 genes. Studies have indicated that SVV $3C^{pro}$ mutants that abrogate Cys and His residues lost protease activity (Qian et al., 2017; Xue et al., 2018). Here, our results indicated that SVV $3C^{pro}$ mutants that abrogate Cys and His residues also lost DUB activity. Therefore, we speculate that the Cys and His residues of SVV $3C^{pro}$ may contribute to both protease and DUB activities. $3C^{pro}$ might suppress type I IFN response by different mechanisms in host cells.

SVV has been identified as a novel oncolytic virus against several human cancers (Burke, 2016). Ubiquitination and deubiquitination are mechanisms that also play important roles in regulation of cancer (Kaushal et al., 2018). Whether SVV can inhibit cancer progression through $3C^{pro}$ DUB activity is still unclear and will need to be investigated in future studies. It may provide a novel method for cancer therapy.

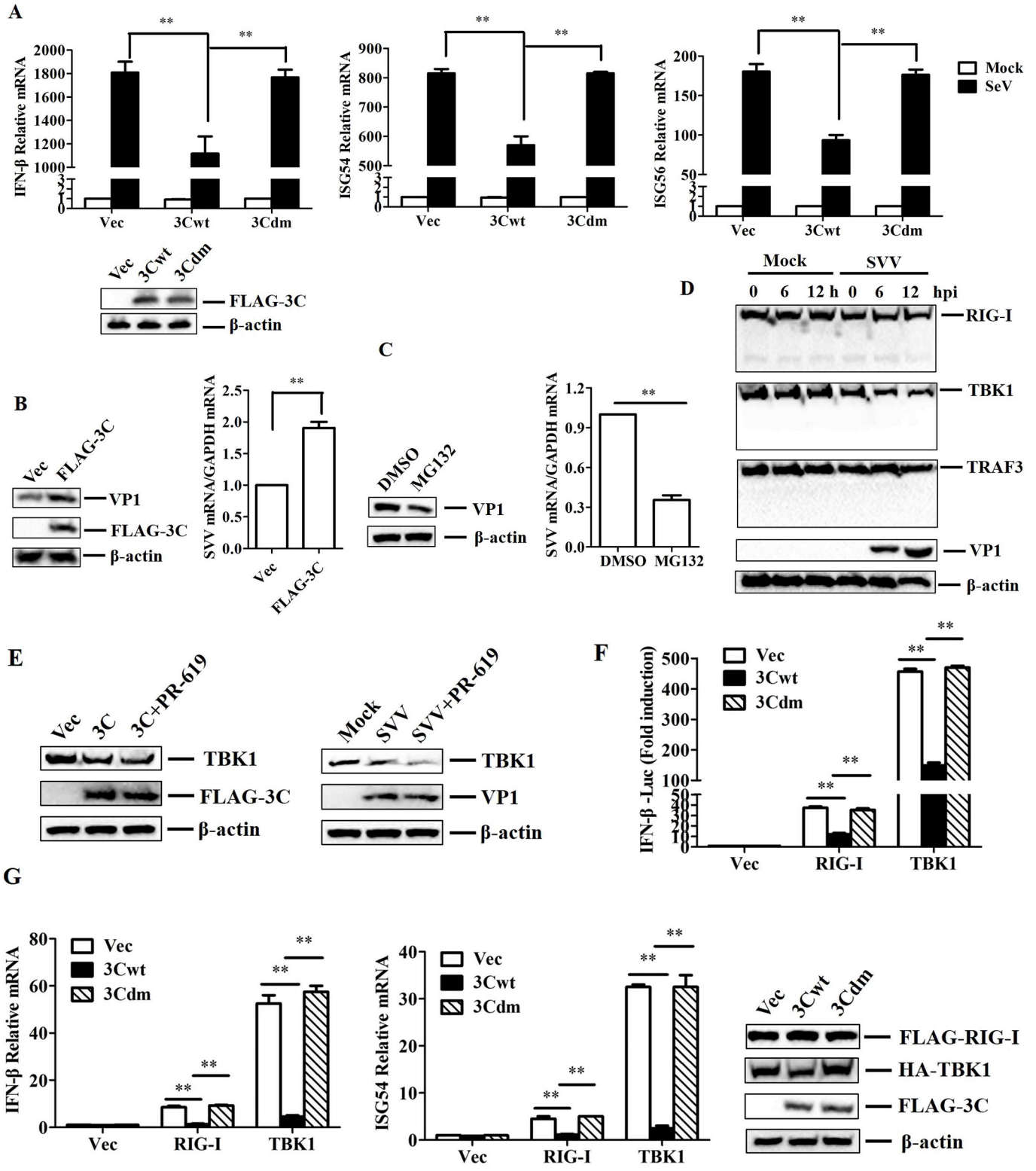

(caption on next page)

Fig. 5. SVV 3C^{pro} inhibits RIG-I- and TBK1-induced type I IFN production. (A) HEK293T cells were seeded in 12-well plates, and the monolayer cells were transfected with 0.5 μg FLAG-3Cwt-expressing plasmid, FLAG-3Cdm-expressing plasmid, or empty vector. At 24 hpt, the cells were mock infected or infected with SeV (100 hemagglutinating activity units) for 12 h. The expression of IFN-β, ISG54, and ISG56 mRNAs was determined with qPCR assay. (B) HEK293T cells were seeded in 6-well plates, and the monolayer cells were transfected with 1 μg FLAG-3C-expressing plasmid or empty vector. At 24 hpt, the cells were infected with an equal amount of SVV (MOI 1) for 12 h. Expression of viral RNA was determined by qPCR assay. Expression of viral VP1 protein was detected by western blotting. (C) HEK293T cells were seeded in 6-well plates, and the monolayer cells were infected with SVV (MOI 1). At 4 hpi, the cells were incubated with or without 20 μM MG132 for 8 h. Expression of viral RNA was determined by qPCR assay. Expression of viral VP1 protein was detected by western blotting. (D) HEK293T cells were seeded in 6-well plates, and the monolayer cells were mock infected or infected with SVV (MOI 1) for 0, 6 and 12 h. Expression of TBK1, RIG-I, TRAF3, and viral VP1 proteins were detected by western blotting. (E) HEK293T cells were seeded in 6-well plates, and the monolayer cells were transfected with 1 μg FLAG–3C-expressing plasmid or infected with SVV (MOI 1). Then, the cells were treated with or without 25 μM PR-619 for 6 h. Cell lysates were analyzed by western blotting. (F) HEK293T cells grown in 24-well plates were co-transfected with 0.1 μg/well of IFN-β-Luc along with 0.01 μg/well of pRL-TK plasmid and 0.1 μg/well of plasmids encoding FLAG-RIG-I, Myc-TBK1, FLAG-3Cwt, FLAG-3Cdm, or empty vector. At 24 hpt, the cells were lysed. The Dual-specific Luciferase Assay kit was used to analyze the luciferase activities of firefly and Renilla. The data represent the means and standard deviations from three independent experiments. (G) HEK-293T cells were seeded in six-well plates, and the monolayer cells were co-transfected with 1 μg FLAG-RIG-I-expressing plasmid, 1 μg FLAG-3Cwt-expressing plasmid, 1 μg FLAG-3Cdm-expressing plasmid, or 1 μg empty vector. The empty vector was used in the transfection process to ensure that the same number of cells received the same amount of total plasmids. Similar transfection were performed for Myc-TBK1 as described above. At 24 hpt, the expression of IFN-β and ISG54 mRNAs was determined with qPCR assay.

Conflicts of interest

The authors declare no competing financial interest.

Acknowledgments

This work was supported by grants from the National Natural Sciences Foundation of China (no. U1501213 and 31672585), the National Key Research and Development Program of China (2016YFD0500901), the Gansu Science Foundation for Distinguished Young Scholars (no. 1606RJDA313) and the Gansu Science Foundation for Young Scholars (1606RJYA280).

Appendix A. Supplementary data

Supplementary data to this article can be found online at https://doi.org/10.1016/j.antiviral.2018.10.028.

References

Altun, M., Kramer, H.B., Willems, L.I., McDermott, J.L., Leach, C.A., Goldenberg, S.J., Kumar, K.G., Konietzny, R., Fischer, R., Kogan, E., Mackeen, M.M., McGouran, J., Khoronenkova, S.V., Parsons, J.L., Dianov, G.L., Nicholson, B., Kessler, B.M., 2011. Activity-based chemical proteomics accelerates inhibitor development for deubiquitylating enzymes. Chem. Biol. 18, 1401–1412.

Barrado-Gil, L., Galindo, I., Martinez-Alonso, D., Viedma, S., Alonso, C., 2017. The ubiquitin-proteasome system is required for African swine fever replication. 12, e0189741.

Burke, M.J., 2016. Oncolytic Seneca Valley Virus: past perspectives and future directions. Oncolytic Virotherapy 5, 81–89.

Casorla-Perez, L.A., Lopez, T., Lopez, S., Arias, C.F., 2017. The Ubiquitin-proteasome System Is Necessary for the Efficient Replication of Human Astrovirus.

Clementz, M.A., Chen, Z., Banach, B.S., Wang, Y., Sun, L., Ratia, K., Baez-Santos, Y.M., Wang, J., Takayama, J., Ghosh, A.K., Li, K., Mesecar, A.D., Baker, S.C., 2010. Deubiquitinating and interferon antagonism activities of coronavirus papain-like proteases. J. Virol. 84, 4619–4629.

Cui, J., Song, Y., Li, Y., Zhu, Q., Tan, P., Qin, Y., Wang, H.Y., Wang, R.F., 2014. USP3 inhibits type I interferon signaling by deubiquitinating RIG-I-like receptors. Cell Res. 24, 400–416.

Fiskin, E., Bionda, T., Dikic, I., Behrends, C., 2016. Global analysis of host and bacterial ubiquitinome in response to Salmonella Typhimurium infection. Mol. Cell 62, 967–981.

Gu, Z., Shi, W., Zhang, L., Hu, Z., Xu, C., 2017. USP19 suppresses cellular type I interferon signaling by targeting TRAF3 for deubiquitination. Future Microbiol. 12, 767–779.

Hales, L.M., Knowles, N.J., Reddy, P.S., Xu, L., Hay, C., Hallenbeck, P.L., 2008. Complete genome sequence analysis of Seneca Valley virus-001, a novel oncolytic picornavirus. J. Gen. Virol. 89, 1265–1275.

Kaushal, K., Antao, A.M., Kim, K.S., Ramakrishna, S., 2018. Deubiquitinating enzymes in cancer stem cells: functions and targeted inhibition for cancer therapy. Drug Discov. Today [Epub ahead of print].

Lin, M., Zhao, Z., Yang, Z., Meng, Q., Tan, P., Xie, W., Qin, Y., Wang, R.F., Cui, J., 2016. USP38 inhibits type I interferon signaling by editing TBK1 ubiquitination through NLRP4 signalosome. Mol. Cell 64, 267–281.

Luo, H., 2016. Interplay between the virus and the ubiquitin-proteasome system: molecular mechanism of viral pathogenesis. Curr. Opin. Virol. 17, 1–10.

Nijman, S.M., Luna-Vargas, M.P., Velds, A., Brummelkamp, T.R., Dirac, A.M., Sixma, T.K., Bernards, R., 2005. A genomic and functional inventory of deubiquitinating enzymes. Cell 123, 773–786.

Okumura, A., Alce, T., Lubyova, B., Ezelle, H., Strebel, K., Pitha, P.M., 2008. HIV-1 accessory proteins VPR and Vif modulate antiviral response by targeting IRF-3 for degradation. Virology 373, 85–97.

Peisley, A., Wu, B., Xu, H., Chen, Z.J., Hur, S., 2014. Structural basis for ubiquitin-mediated antiviral signal activation by RIG-I. Nature 509, 110–114.

Qian, S., Fan, W., Liu, T., Wu, M., Zhang, H., Cui, X., Zhou, Y., Hu, J., Wei, S., Chen, H., Li, X., Qian, P., 2017. Seneca Valley virus suppresses host type I interferon production by targeting adaptor proteins MAVS, TRIF, and TANK for cleavage. J. Virol. 91.

Raaben, M., Posthuma, C.C., Verheije, M.H., te Lintelo, E.G., Kikkert, M., Drijfhout, J.W., Snijder, E.J., Rottier, P.J., de Haan, C.A., 2010. The ubiquitin-proteasome system plays an important role during various stages of the coronavirus infection cycle. J. Virol. 84, 7869–7879.

Schmittgen, T.D., Livak, K.J., 2008. Analyzing real-time PCR data by the comparative C(T) method. Nat. Protoc. 3, 1101–1108.

Segales, J., Barcellos, D., Alfieri, A., Burrough, E., Marthaler, D., 2017. Senecavirus A. Veterinary pathology. 54, 11–21.

Song, G., Liu, B., Li, Z., Wu, H., Wang, P., Zhao, K., Jiang, G., Zhang, L., Gao, C., 2016. E3 ubiquitin ligase RNF128 promotes innate antiviral immunity through K63-linked ubiquitination of TBK1. Nat. Immunol. 17, 1342–1351.

Sun, Z., Chen, Z., Lawson, S.R., Fang, Y., 2010. The cysteine protease domain of porcine reproductive and respiratory syndrome virus nonstructural protein 2 possesses deubiquitinating and interferon antagonism functions. J. Virol. 84, 7832–7846.

van Wijk, S.J.L., Fricke, F., Herhaus, L., Gupta, J., 2017. Linear ubiquitination of cytosolic Salmonella Typhimurium activates NF-kappaB and restricts bacterial proliferation. 2, 17066.

Wang, C., Chen, T., Zhang, J., Yang, M., Li, N., Xu, X., Cao, X., 2009. The E3 ubiquitin ligase Nrdp1 'preferentially' promotes TLR-mediated production of type I interferon. Nat. Immunol. 10, 744–752.

Wang, D., Fang, L., Li, P., Sun, L., Fan, J., Zhang, Q., Luo, R., Liu, X., Li, K., Chen, H., Chen, Z., Xiao, S., 2011. The leader proteinase of foot-and-mouth disease virus negatively regulates the type I interferon pathway by acting as a viral deubiquitinase. J. Virol. 85, 3758–3766.

Wang, S., Liu, H., Zu, X., Liu, Y., Chen, L., Zhu, X., Zhang, L., Zhou, Z., Xiao, G., Wang, W., 2016. The ubiquitin-proteasome system is essential for the productive entry of Japanese encephalitis virus. Virology 498, 116–127.

Wu, Q., Zhao, X., Chen, Y., He, X., Zhang, G., Ma, J., 2016. Complete genome sequence of Seneca Valley virus CH-01-2015 identified in China. Genome Announc. 4.

Xue, Q., Liu, H., Zhu, Z., Yang, F., Ma, L., Cai, X., Xue, Q., Zheng, H., 2018. Seneca Valley Virus 3C(pro) abrogates the IRF3- and IRF7-mediated innate immune response by degrading IRF3 and IRF7. Virology 518, 1–7.

Zhao, X., Wu, Q., Bai, Y., Chen, G., Zhou, L., Wu, Z., Li, Y., Zhou, W., Yang, H., Ma, J., 2017. Phylogenetic and Genome Analysis of Seven Senecavirus a Isolates in China.

Zhu, Z., Yang, F., Chen, P., Liu, H., Cao, W., Zhang, K., Liu, X., Zheng, H., 2017. Emergence of novel Seneca Valley virus strains in China. 64, 1024–1029 2017.